

## Characterisation of Low Reynolds Number Fountain Behaviour

Williamson, N.<sup>1</sup>, Srinarayana, N.<sup>1</sup>, Armfield, S.W.<sup>1</sup>, McBain, G.<sup>1</sup> and Lin, W.<sup>2</sup>

<sup>1</sup>School of Aerospace, Mechanical and Mechatronic Engineering  
The University of Sydney, NSW, 2006 AUSTRALIA

<sup>2</sup>School of Engineering  
James Cook University, Townsville, Queensland, 4811 AUSTRALIA

### Abstract

Experimental evidence for previously unreported fountain behaviour is presented. It has been found that the first unstable mode of a wall bounded three dimensional round fountain is a laminar flapping motion that can grow to a circling or multi-modal flapping motion. With increasing Froude and Reynolds numbers, fountain behaviour becomes more disorderly, exhibiting a laminar bobbing motion. The transition between steady behaviour, the initial flapping modes and the laminar bobbing flow can be approximately described by a function  $C = FrRe^{2/3}$ . The transition to turbulence occurs at  $Re > 120$ , independent of Froude number. For  $Fr > 20$  and  $Re \lesssim 120$ , sinusoidal shear instabilities have been observed in the rising fluid column. For  $Re > 120$  these instabilities cause the fountain to intermittently breakdown into turbulent jet like flow. A regime map of the fountain behaviour for  $0.7 < Fr < 55$  and  $15 < Re < 1100$  is presented and the underlying mechanisms for the observed behaviour are proposed.

### Introduction

Fountains (negatively buoyant plumes) occur when a fluid is injected into another fluid of differing density where the buoyancy force opposes the momentum flux. The injected fluid penetrates a distance into the environment before falling back around itself. There have been numerous studies investigating fountain behaviour in a variety of configurations including round fountains [1], planar fountains, fountains impinging on a solid surface and fountains penetrating an interface [2]. Fountain flow may be categorised as weak or forced, depending on the ratio of buoyancy and momentum flux and also as laminar or turbulent. In general, fountain behaviour can be characterised by the Froude and Reynolds numbers, where  $Fr = U_o / \sqrt{gR_o(\rho_o - \rho_f) / \rho_f}$  and  $Re = U_o R_o / \nu_o$ . In this study the subscript  $o$  indicates a quantity at the fountain source and  $f$  indicates a property of the ambient fluid.

Most early studies have focused on turbulent fountains with significant contributions by Morton [3], Turner [1], Mizushima *et al.* [4], Campbell and Turner [5] and Baines *et al.* [6]. The consensus in these works, on both dimensional, analytical and experimental grounds, is that for turbulent fountains the maximum penetration depth scales as  $Z_m/R_o = CFr$  and is Reynolds number independent. Turner [1] and then Campbell and Turner [5] found  $C = 2.46$  from experiments. Baines *et al.* [6] extended Turner's experimental work to  $10 < Fr < 300$  at  $Re \sim 2000$ , confirming the scaling. Abraham [7] proposed an analytical solution finding  $C = 2.74$  and Mizushima *et al.* [4] experimentally obtained  $C = 2.35$  for  $5 < Fr < 260$  and  $1130 < Re < 2710$ . Pantzlauff and Lueptow [8] experimentally examined turbulent fountains with  $15 \leq Fr \leq 78$  and  $1250 \leq Re \leq 7500$  finding  $C = 2.1$ .

More recently attention has been given to turbulent weak fountains [11, 12, 2, 9], transitional fountains [13] and laminar foun-

tains [10]. Zhang and Baddour [9] examined low and high Froude number round fountains and found that for  $Fr < 7$  the mean penetration height no longer scales linearly with  $Fr$  and is better represented by  $Z_m/R_o = CFr^{1.3}$  where  $C = 1.7$ . For  $Fr > 7$  they found  $Z_m/R_o = 3.06Fr$ .

Lin and Armfield [11] numerically simulated weak fountains with  $0.2 \leq Fr \leq 1.0$  and found a linear scaling valid with  $Z_m/R_o \sim Fr$ . The authors extended the study in [12], and found that for very weak fountains with  $0.0025 \leq Fr \leq 0.2$  and  $Re = 200$ ,  $Z_m/R_o \sim Fr^{2/3}$ . The authors also tested the effects of viscosity and found that for  $5 \leq Re \leq 800$ , with  $Fr = 0.05$ ,  $Z_m/R_o \sim (Re)^{-2/3}$ .

Philippe *et al.* [10] present an experimental examination of laminar fountains for  $1 \lesssim Fr \lesssim 200$  and  $0 < Re < 80$ . The authors describe very steady fountains which exhibit no oscillation and eventually reach a steady state maximum penetration. The authors find that viscosity is significant for  $Re \lesssim 50$ , and the penetration height scales with  $Z_m/R_o = CFrRe^\phi$  where  $\phi \sim 0.5 - 0.6$ . The authors performed additional tests for  $60 < Re < 250$  and found that the effect of viscosity becomes less important and the scaling for the penetration height approaches the relation of Turner [1].

Lin and Armfield [13] examined the behaviour of transitional fountains for  $1 \leq Fr \leq 8$  and  $200 \leq Re \leq 800$  using an axisymmetric numerical simulation. The authors found that in this range, viscosity becomes important and the mean height scales like  $FrRe^{1/4}$ .

Kaye and Hunt [14] present experimental and analytical evidence that the rise height for weak fountains scales with  $Z_m/R_o \sim Fr$  for  $Fr \gtrsim 3.0$ ,  $Z_m/R_o \sim Fr^2$  for  $1.0 \lesssim Fr \lesssim 3.0$  and  $Z_m/R_o \sim Fr^{2/3}$  for  $Fr \lesssim 1.0$ .

There is very clear agreement in literature that for high Froude number turbulent fountains, the mean height scales linearly with the Froude number. The behaviour of low Reynolds number laminar and transitional fountains is less well understood, with a wide range of scaling relations reported for the fountain penetration height. It is clear from previous work however that high Reynolds number scalings do not universally apply to laminar and transitional flows and that viscosity cannot be ignored in this region. In addition the nature of the flow behaviour in this region is not well described.

In this work the nature of laminar and transitional fountain flow is investigated experimentally. It has been found that several distinct types of fountain behaviour exist that have not been reported in the literature. Using these observations a regime map has been constructed locating transition regions between types of flow behaviour. These observations indicate that the dominant mechanisms present in the flow differ dramatically with Froude and Reynolds number.

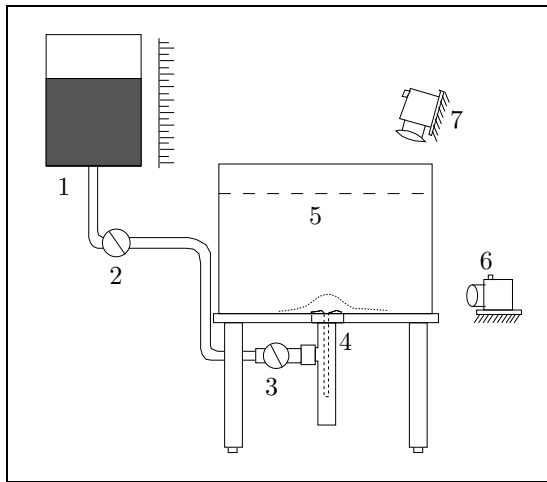


Figure 1: Schematic representation of fountain experimental setup with 1:header tank, 2:on/off valve, 3:flow control valve, 4:inlet nozzle, 5:fresh water tank, 6-7:digital cameras.

### Experimental Setup

Experiments have been performed by injecting salt water up into a fresh water tank, 25cm deep with 34cm square base. The saline water is fed from a header tank to the base of the fresh water tank as shown in the arrangement figure 1. The water is injected from a sudden start and maintained at a constant flow rate throughout the experiment. During an experiment the saline fluid rises and then falls back on itself and finally spreads along the base of the fresh water tank. The problem is similar to the filling box problem of Turner [1] and Baines *et al.* [6] but in this study the long term behaviour of the fountain as the tank fills up is not of interest and the experiment is stopped before the saline water reaches the walls of the tank. Additionally, in this study the inlet pipe is aligned flush with the bottom of the fresh water tank unlike many previous investigations [1, 5, 6, 10] where a re-entrant nozzle was used. To the authors knowledge the only previous studies of round fountains using this configuration are the numerical studies of Lin and Armfield [11, 12, 13] and the experimental work of Pantzlauff and Lueptow [8], however in many papers the experimental arrangement is unclear. This configuration may be significant for low Froude number behaviour.

The fountain inlet flow rate, inlet pipe diameter and the salinity of the inlet fluid were varied to cover a wide range of Reynolds and Froude numbers. The volume flow rate varied from  $0.06\text{cm}^3/\text{s}$  to  $11\text{cm}^3/\text{s}$ . Nozzle diameters of 4.80mm, 2.54mm, 1.66mm and 1.13mm were used. The ratio of inlet pipe length to pipe diameter was greater than 40 in each case, ensuring that the flow is fully developed as it enters the tank. The density ratio is varied with  $0.004 < \Delta\rho/\rho_f < 0.16$ , where  $\Delta\rho = \rho_o - \rho_f$ . The salinity also effects the solution viscosity and in this work has values  $1.01 \times 10^{-6} < \nu_o < 1.4 \times 10^{-6}$  such that  $\nu_o \leq 1.4\nu_f$ . The characteristic velocity used in the Reynolds number and Froude number is defined as  $U_o = Q_o/A_o$ , where  $Q_o$  is the volume flow rate of the saline fluid in the pipe and  $A_o$  is the cross-sectional area of the pipe.

Small concentrations of dye were used as the tracer in the saline water. The effect of the dye on the solution density was taken into account. The flow was recorded on two digital cameras at 15 frame/second with experiments running for less than 2 minutes or until the saline water front reaches the edge of the tank.

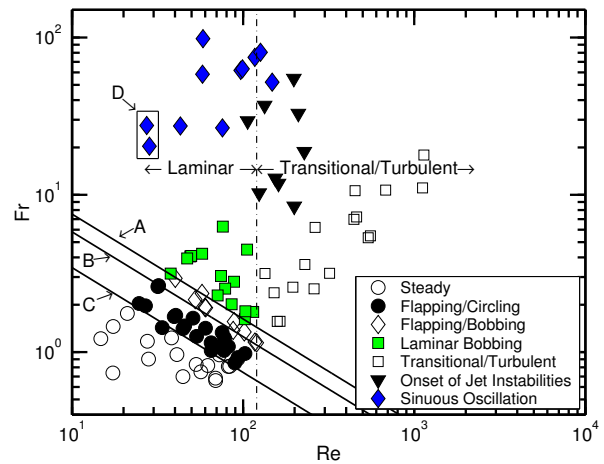


Figure 2: Regime map of fountain behaviour with Re and Fr. Solid lines  $C = FrRe^{2/3}$  where the constant C is - A:35, B:27, C:16.

### Observations

The experiments were performed over the range  $0.7 < Fr < 100$  and  $15 < Re < 1100$  and the fountain behaviour observed placed on a regime map of Froude and Reynolds numbers in figure 2. Broadly the flow can be categorised as laminar for  $Re < 120$ , with the transition to turbulence occurring above this region independent of Froude number. No turbulence statistics were taken so these observations are purely visual. Within both the laminar and transitional regions, a number of other sub-groupings have been made which are described below.

In the laminar region for  $Fr < 10$ , a range of behaviour is observed that has both Reynolds and Froude number dependence. The flow has been categorised into steady, flapping/circling, transitional bobbing/flapping and finally laminar bobbing regions. The demarcation lines between different laminar fountain behaviour are found to be well described by  $C = FrRe^{2/3}$  for  $30 < Re < 120$  and  $0.5 < Fr < 10$ , as shown in figure 2.

The laminar steady region is observed for  $0 < Fr < 16Re^{-2/3}$  and for the range of Reynolds numbers examined in this study. In this region the flow is stable with no fluctuation in fountain height and is similar to the weak fountains examined by Lin and Armfield [11, 12].

Between  $16Re^{-2/3} < Fr < 27Re^{-2/3}$  the flow becomes unstable resulting in several interesting modes of oscillation. The first mode of oscillation is a two dimensional flapping motion. This usually but not always develops into a flapping mode whereby the plane of flapping rotates about the fountain axis, so the direction of flapping changes. This behaviour then develops into a circling or multi-modal flapping motion where the maximum height of the fountain circles around the fountain axis. In many cases the fountain was observed to continually switch between the different flapping/circling modes described here.

In the laminar bobbing region the fountain behaviour is highly unsteady and three dimensional. It is characterised by the fluctuation in fountain height, as the fountain front continually rises, stagnates and then collapses around the next rising front. A distinct difference between this behaviour and the flapping/circling modes, is that with the bobbing motion, the fountain height is always at a maximum in the centre of the fountain axis whereas for the flapping or circling modes, the location of maximum fountain height is always off-axis. On the regime plot in figure 2, this region occurs for  $35Re^{-2/3} < Fr \lesssim 10$ . Between the flap-

ping motion and the bobbing motion there is a transition region for  $27Re^{-2/3} < Fr < 35Re^{-2/3}$ , where both behaviours can be observed alternatively or together.

At higher Froude numbers in the laminar region ( $20 < Re < 120$  and  $Fr \gtrsim 20$ ), the fountain behaviour appears to be fundamentally different. The fluid column rises to a much greater height and the flow is also characterised by a broad fountain head, where the stagnating fountain fluid is spread horizontally a short distance before reversing back on the rising column. Instead of collapsing on the rising column like the laminar bobbing flow, the reversing fluid flows down around the rising column.

A peculiar and very interesting phenomena occurs at low Reynolds numbers and high Froude numbers in this region. The fluid falling back towards the source flows in a laminar cylindrical sheet entirely enveloping the rising fluid column and trapping ambient fluid inside. This trapped fluid is slowly advected out over what appears to be a time-scale related to the diffusion of momentum. When the fluid is entirely advected away, the rising and falling fluid come in direct contact, the shear force acting on the rising column is increased and the fountain height is then reduced. The runs in which this behaviour has been observed have been indicated in figure 2 by the region marked *D*.

For all the points in the region defined by  $20 < Re < 120$  and  $Fr \gtrsim 20$ , the interaction between the descending fluid and the rising fluid column appears responsible for several other interesting phenomena. At low Reynolds number an intermittent sinuous instability is observed, appearing as a wave travelling up the fluid column. This leads to a slight 'wobbling' of the fountain head. At higher Reynolds number the sinuous instability is manifested more strongly. When the waves reach the head of the fountain and the stagnating/reversing fluid, the amplitude increases and column appears to periodically buckle at the head. This leads to an increase in flow falling around this rising column and a corresponding increase in shear. This sometimes but not always results in partial collapse of the fountain.

In the same range of Froude numbers ( $Fr \sim 20 - 100$ ), as the Reynolds number is increased into the transitional/turbulent region in figure 2, the sinuous instability appears to intermittently breakdown into a turbulent jet like flow at some point along the rising fluid column. The location of this point moves up and down the rising fluid column and, as with the sinuous instability in the laminar region, this appears to be initiated by a shear interaction between the rising column and the descending fluid. This instability results in major fountain collapse events leading to large oscillations in the fountain penetration height. This instability is most clear in the points grouped as 'Onset of Jet Instabilities', where the flow is not very turbulent and both the sinuous instabilities and the jet like break down are observed together. The same type of periodic collapse and rise behaviour of the fountain has also been observed clearly in most of the transitional/turbulent region, up to  $Re \sim 1100$ , the limit of the experiments in this study. The behaviour is clearer in the high Froude number cases than the low Froude number cases where the fountains have a low penetration height and the frequency of oscillation is very high. The mechanism driving the oscillation in the height of the low Froude number transitional/turbulent fountains may be instead related to the mechanism driving the oscillation in the laminar bobbing flow, but this is very difficult to diagnose visually from the experiments.

## Discussion

In all of the unsteady regions some form of oscillation in fountain height was observed. The spectra of frequencies from the time series of fountain height has been examined. The dominant

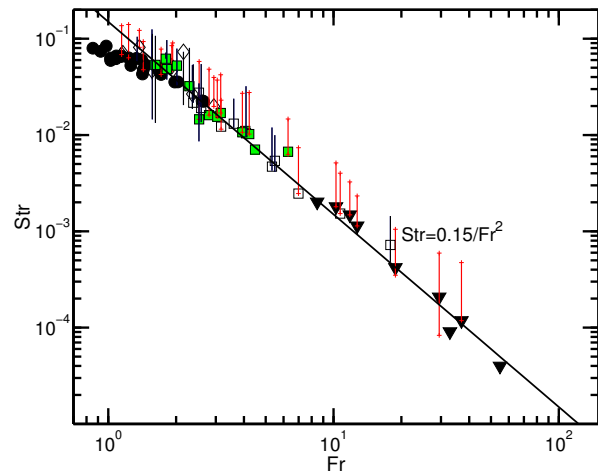


Figure 3: Strouhal number for primary mode of oscillation in height, marked with symbols defined in figure 2. Black vertical lines indicate range of frequencies present for multimodal flows. Limits of red vertical lines indicate secondary frequencies if present.

modes of oscillation have been plotted in figure 3, as Strouhal number against Froude number where the Strouhal number is  $Str = Uo/fR_o$  and  $f$  is frequency in Hz. Where secondary frequencies present, these have been marked on the plot.

For the flapping and circling cases, this frequency corresponds to that of the flapping/circling. For the fountains at Froude and Reynolds numbers grouped as 'Onset of Jet Instabilities', 'Transitional/Turbulent' or as 'Laminar Bobbing' in figure 2, the primary frequency corresponds to the frequency of major fountain collapse.

The flapping/bobbing transition region is characterised by multi-modal bobbing/flapping and picking a dominant mode is very interpretative. In these regions the range of frequencies present are marked in figure 3 by dark lines. The cases marked as 'Sinuous Oscillation' have been excluded as the oscillation in height in this region is unclear and irregular.

The dominant modes for the laminar bobbing flow and the flow in the transitional/turbulent region all collapse onto a single line of  $Str = c/Fr^2 = cRi$ , where  $Ri$  is the Richardson number. This suggests that the mechanism behind the dominant features of the flow may be related. The flapping and transitional flapping/bobbing fountains appear to depart from the  $Str \sim Ri$  line at low Froude numbers. In this region the curve appears to approach a line of constant Strouhal number and may have an additional Reynolds number dependency. Friedman [2] noted that above  $Fr \sim 1$ , round fountains (using a re-entrant nozzle) become unstable with the fountain rising and collapsing in a periodic manner. The author found that this behaviour was well described by a line of constant Strouhal number,  $Str = 0.16$  for  $1.0 < Fr < 3.16$ . For  $Fr > 3.16$  the fountain behaviour was noted to be more unpredictable with a less consistent frequency of oscillation.

Preliminary numerical and experimental results performed by the present authors for planar fountains suggest that the flapping modes observed in this study only occur for flush wall mounted nozzles, not re-entrant nozzles. This suggests that this behaviour may be related to the presence of a bounding wall or the intrusion formed.

The scaling for the mean maximum penetration height is very

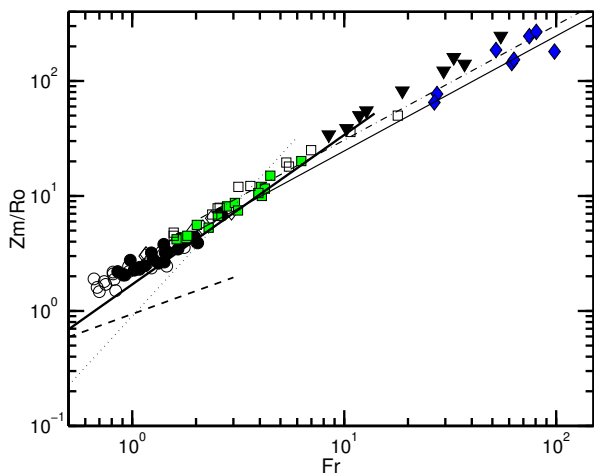


Figure 4: Dimensionless mean maximum penetration height as function of Froude number. Symbols defined in figure 2. Dashed line:  $0.94Fr^{2/3}$  [14], dotted line:  $0.9Fr^2$  [14], thin solid line:  $2.46Fr$  [1], thick solid line:  $1.7Fr^{1.3}$  [9] and thin dashed-dotted line:  $3.06Fr$  [9].

usefull for investigating fountain behaviour since so many previous authors have made contributions to this subject. The mean fountain height for all the experiments in this study are plotted in figure 4 against Froude number, with the high Reynolds number scaling of Turner [1], the two low Froude number scaling relations of Kaye and Hunt [14] and the two relations of Zhang and Baddour [9]. None of the previous relations is a very good fit to the data. In particular, the fit of the low Froude number relations is especially poor. This could potentially be due to a Reynolds number effect or the influence of the lower tank boundary wall on the flow. Neither Kaye and Hunt or Zhang and Baddour make clear if their study used a re-entrant nozzle or make clear the range of Reynolds number used.

The two previous studies on laminar and transitional fountains, Philippe *et al.* [10] and Lin and Armfield [13] found the scaling for the mean fountain height is still linear in the Froude number but contains an additional Reynolds number dependence. The functional dependence of the linear Froude number scaling on Reynolds number for the results in this study can be seen in figure 5 where the quantity  $Zm/FrRo$  is plotted. Our data is not well fitted by either  $0.5 < \phi < 0.6$  or  $\phi = 0.25$ . At very low Froude numbers, the results here are unclear. As noted by Philippe *et al.*, at higher Reynolds number the quantity  $Zm/FrRo$  approaches the value of 2.46 first noted by Turner [1]. Unfortunately, the experimental rig in this study is limited to  $Re < 1100$ , compared with the studies by Turner and colleagues at  $Re > 2000$ , so this cannot be confirmed. It does suggest however that fountain flow is not fully turbulent even at  $Re = 1100$ .

### Conclusions

The behaviour of low Reynolds number fountain flow has been investigated experimentally and found to strongly depend on both Froude number and Reynolds number. Relations have been proposed which separate distinct types of fountain behaviour on a Reynolds number and Froude number plane.

Across a wide range of Reynolds and Froude numbers similarities in behaviour have been noted. High Froude number fountains appear strongly dominated by a shear interaction between the rising and falling flow. At low Reynolds number this interaction appears responsible for a sinuous instability ob-

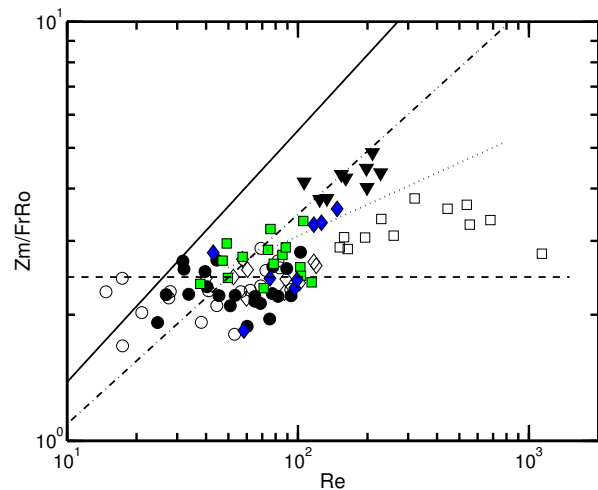


Figure 5: Constant for Froude number scaling with Reynolds number,  $c = Zm/FrRo$ . Symbols defined in figure 2. Dashed line:  $2.46$  [1], solid line:  $0.347Re^{0.6}$  [10], dashed-dotted:  $0.347Re^{0.5}$  [10], dotted line:  $0.974Re^{0.25}$  [13].

served in the fountain column. At higher Reynolds number, this sinuous instability intermittently causes the fountain column to break down into turbulent jet like flow. For  $Fr \lesssim 10$ , fountain behaviour is characterised by the interaction between the falling fountain front and the new rising fountain leading to bobbing and flapping behaviour. In the bobbing, and turbulent/transitional regions, the frequency of oscillation in fountain height appears to be related by a function of  $Str = cRi$ , indicating a possible common mechanism behind the behaviour observed.

It is clear from the scaling of the fountain penetration height that the mechanisms behind transitional and laminar fountains are more complex than those for turbulent fountains which have received more attention to date.

### Acknowledgements

The authors wish to acknowledge the support of the Australian Research Council.

### References

- [1] Turner, J. S., Jets and plumes with negative or reversing buoyancy, *J. Fluid Mech.*, **26**, 1966, 779–792.
- [2] Friedman, P.D., Oscillation height of a negatively buoyant jet, *J. Fluids Eng.-Trans. ASME*, **128**, 2006, 880–882.
- [3] Morton, B. R., Forced Plumes, *J. Fluid Mech.*, **5**, 1959, 151–163.
- [4] Mizushima, T., Ogino, F., Takeuchi, H. and Ikawa, H., An experimental study of vertical turbulent jet with negative buoyancy, *Wärme-und Stoffübertragung*, **16**, 1982, 15–21.
- [5] Campbell, I. H. and Turner, J. S., Fountains in magma chambers, *J. Petrol.*, **30**, 1989, 885–923.
- [6] Baines, W.D., Turner, J. S. and Campbell, I. H., Turbulent fountains in an open chamber, *J. Fluid Mech.*, **212**, 1990, 557–592.
- [7] Abraham, G., Jets with negative buoyancy in homogeneous fluid, *J. Hyd. Res.*, **5**, 1967, 235–248.

- [8] Pantzloff, L. and Lueptow, R.M. Transient positively and negatively buoyant turbulent round jets, *Exp. Fluids*, **27**, 1999, 117–125.
- [9] Zhang, H. and Baddour, R. E., Maximum penetration of vertical round dense jets at small and large Froude numbers, *J. Hydraulic Eng.*, **124**, 1998, 550–553.
- [10] Philippe, P., Raufaste, C. Kurowski, P. and Petitjeans, P., Penetration of a negatively buoyant jet in a miscible liquid, *Phys. Fluids.*, **17**, 2005, 1–10.
- [11] Lin, W. and Armfield, S. W., Direct simulation of weak axisymmetric fountains in a homogeneous fluid, *J. Fluid Mech.*, **403**, 2000, 67–88.
- [12] Lin, W. and Armfield, S. W., Very weak axisymmetric fountains in a homogeneous fluid, *Numer. Heat Transfer A*, **38**, 2000, 377–396.
- [13] Lin, W. and Armfield, S. W., Direct simulation of fountains with intermediate Froude and Reynolds numbers, *ANZIAM J.*, **45**(E), 2004, C66–C77.
- [14] Kaye, N.B. and Hunt, G.R., Weak fountains, *J. Fluid Mech.*, **558**, 2006, 319–328.